Body Imaging at 7 Tesla with Multichannel Transmit Capability

K. Ugurbil[1]; J.T. Vaughan[1]; G.J. Metzger[1]; P.-F. van de Moortele[1]; C.J. Snyder[1]; L. DelaBarre[1]; P. Bolan[1]; E Auerbach[1]; P. Weale[2]; S. Zuehlsdorff[2]; S. Nielles-Vallespin[2,3]; R. Jerecic[2]

[1]*Center for Magnetic Resonance Research (CMRR), Dept. of Radiology, University of Minnesota, Minneapolis, USA*
[2]*Siemens Healthcare*
[3]*Current address: Royal Brompton Hospital, London, UK*

In the last two decades, a plethora of magnetic resonance (MR) techniques, such as functional magnetic resonance imaging (fMRI), have come to play an indispensable role in the neurosciences. In our laboratory, the Center for Magnetic Resonance Research (CMRR) at the University of Minnesota, the evolution of such methods has been intricately tied with the development of high field MR, starting with the installation of one of the first three 4 Tesla (T) scanners in approximately 1990, followed by the establishment of the very first 7 Tesla system in 1999 (e.g. reviews [1–5]).
The development of this 7T scanner for human imaging was justified based on the results of numerous human and animal model studies conducted at 4 and 9.4T, respectively, in our lab through the mid-nineties. These studies demonstrated that despite many contravening notions of the time, high magnetic fields could provide significant advantages. Using this first ultra-high[1] field 7T system, we were able to demonstrate that challenges faced at such field strengths in human imaging could be overcome. Although it is taken for granted today, at the time we started working with 7T, even field-dependent signal-to-noise ratio (SNR) gains in the human head were questioned. In one of first 7T studies, however, we were able to experimentally demonstrate for the first time that SNR does increase with magnetic field in the human head, though this increase was complex and spatially non-uniform [6]. More importantly, over the years, 7T has been shown to provide unique anatomical, functional and physiologic information beyond just gains in SNR (e.g. [7–11]). With the rapidly increasing number of recent 7T installations, demonstration of such unique uses of ultra-high fields is also rapidly blooming.
For approximately a decade, 7T studies were restricted to the human head. Ever since the discouraging early 4T results from manufacturers' laboratories [12], the human torso has been considered too difficult to tackle at ultra-high fields. The large B_1 and signal intensity inhomogeneities noted in these early 4T head and body images were ascribed to "dielectric resonances". However, some of the first experiments we conducted at 7T to understand the RF behavior in the human body at the proton Larmor frequency at this field strength (300 MHz) indicated that we are not dealing with a "resonance" phenomenon. Rather, in a paper we and our collaborators from Penn State University published in 2001 [13], we concluded that 300 MHz RF behaves as a damped traveling wave in the human body and that (to quote from our original paper) "the characteristic image intensity distribution in the human head is the result of spatial phase distribution and amplitude modulation by the interference of the RF traveling waves determined by a given sample-coil configuration". Later studies further confirmed that when the object size exceeds the wavelength of the RF used, we operate in the damped traveling wave regime, leading to large and spatially rapid phase variations over the object, resulting in destructive interferences [14] and these destructive interferences are responsible for the spatially non-uniform SNR gains that was noted in our earlier study [6]. This was in fact good news: Resonance phenomena are difficult to deal with for recovering signal where there is virtually none; but destructive interferences due to traveling waves can be managed to extract full SNR gains intrinsically provided by increasing magnetic fields.
This complex RF behavior at ultra-high fields in fact turns out to be a major advantage for signal reception, leading to significantly better parallel imaging performance on the receive side at 7T or above. Thus, as the magnetic field increases, spatial encoding information provided by the receive array replaces k-space data to a larger extend due to the complex RF phase and amplitude over the sample [15–17]. However, the consequences of damped traveling wave behavior is a major problem on the transmit side and it is particularly severe in the human body where the object size is 4 to 6 (or more) times larger than the 300 MHz wavelength, which is ~12 cm in human tissues such as muscle and brain.

Figure 1 illustrates electro-dynamic simulations taken from our recent paper [18] for the human body at 7T: The RF field and SAR were modeled by the finite difference time domain (FDTD) method, for a "body" coil at 7T with and without the human body loading the coil.
The circularly polarized transmit B_1 (i.e. B_1^+) field magnitude generated in the unloaded body coil shown in figure 1 was *uniform* in a cylindrical volume with a length slightly less than the length of the resonant elements in this coil (33 cm). The axial plane shown in figure 1 (top row, left) is for a slice in the center of this volume. Despite the uniformity of B_1^+ in the *unloaded* coil, upon loading with a human body, the magnetic field and consequently power deposition becomes extremely non-uniform (Fig. 1, lower part). There are regions in the center of the body where there is virtually no RF (light blue color). Note that highest intensity of the B_1^+ and the largest SAR is in the human head, even though the head is significantly outside the coil and that when unloaded the coil does not have any significant B_1^+ in the region where the head is.
Our solution to the destructive interferences induced by traveling waves has been the use of multichannel parallel transmit (pTx) with channel-specific independent control [19–22, 18]. With this approach, the B_1^+ fields can be targeted and homogenized over a predefined region, enabling body imaging for the first time in the human torso at 7T [23, 24, 18]. The strategy is not to aim for a homogeneous image over the entire slice but rather over the targeted organ. Figure 2 illustrates the cardiac set-up, the B_1^+ distribution before and after B_1^+ optimization over the heart (images in color) and the resultant cardiac image at 7T. In this approach, we employ a dual 8-channel transmit and receive array placed one above and one below the human torso for a total of 16 transmit and receive elements (Fig. 2). Excellent quality cardiac images were also obtained using a more traditional circumscribing TEM body coil

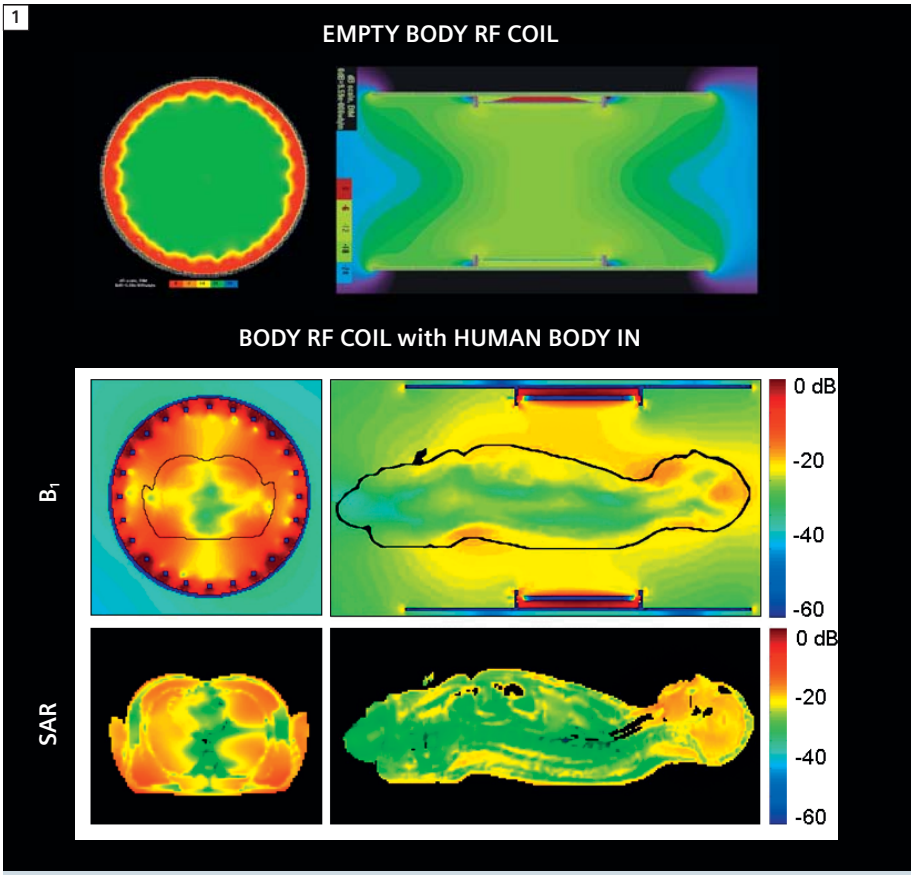

1 B_1 and SAR calculations for a TEM Body RF coil tuned to 300 MHz with and without the human body in the coil. The body model used was derived from the National Library of Medicine (NLM) Visual Human digital atlas whose segmented anatomy was adjusted to match the conductivity and permittivity of tissues at 300 MHz. The coil was driven at four ports (45°, 135°, 225°, and 315°).

but driven as a 16-channel transmit and receive array [18]. Two cardiac imaging examples from such a body coil are illustrated in figure 3. Functional cardiac cines of these and other cardiac images can be found at http://www.cmrr.umn.edu/research/videos/. We have had similar success with imaging the prostate [23] and the kidney (unpublished results), demonstrating the feasibility of excellent high resolution torso imaging at 7T (Fig. 3).
So far, we have employed multichannel transmit only for "B_1^+shimming" but not for generating spatially targeted pulses (e.g. [25–28]) using transmit SENSE principles [29, 30]. In the B_1^+shimming approach, all pTx channels transmit the same RF pulse waveform but with differing phases and/or amplitudes. This approach is particularly suitable in body imaging where the targeted organ is often much smaller then the dimensions of the torso, which dictates the dimensions of the RF transmit array to be used. When the target covers a small portion of the entire field of view, optimizing the B_1^+ over this target in fact results in decreases in power deposition (SAR) [23], which is a major confound at ultra-high field applications. Spatially tailored pulses, on the other hand rely on different modulation patterns on each channel, which can be generated on the Siemens pTx system. Such pulses have been known

[1] The radiofrequency band 300 MHz to 3 GHz is defined as Ultra high frequency (UHF) (see http://en.wikipedia.org/wiki/Ultra_high_frequency). The hydrogen nucleus resonance frequency at 7T is 300 MHz i.e. in UHF band. Therefore, 7T to 70T can be defined as Ultra High Field (UHF).

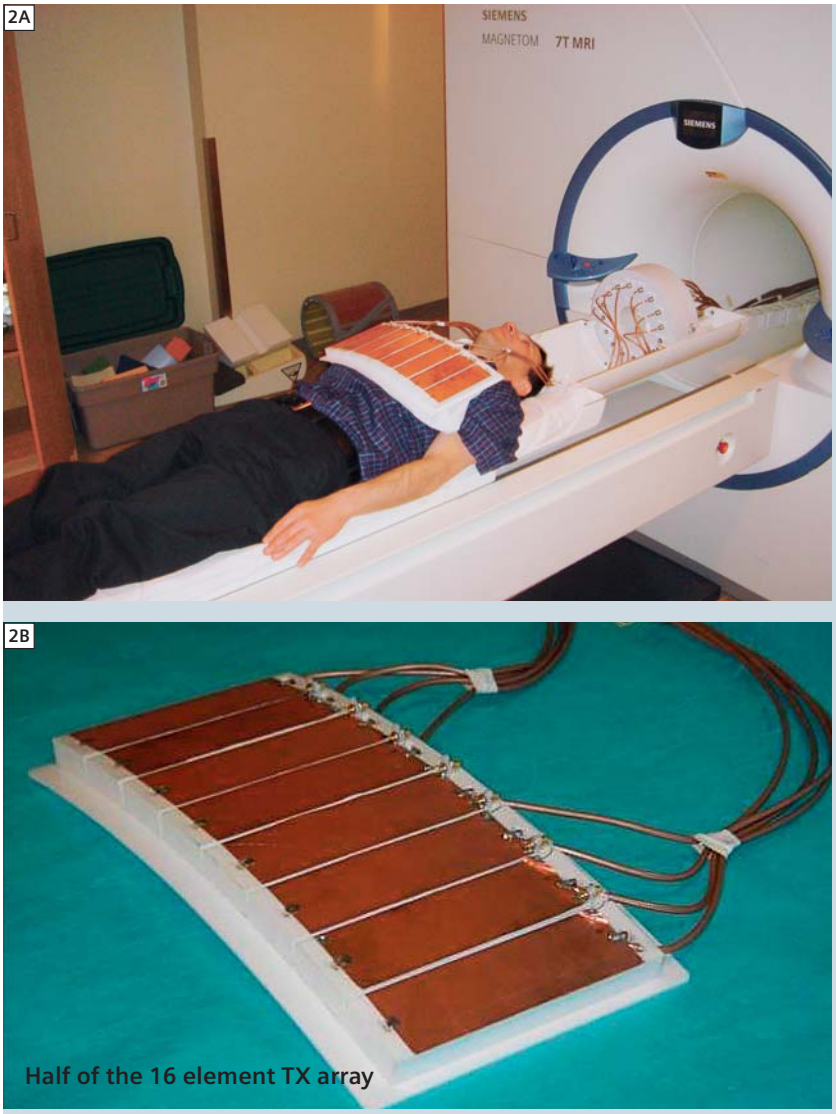

2 The multichannel transmit and receive array coil that is used for body imaging at 7T. Only the 8 elements positioned superior to the subject are shown. An identical unit is placed below the subject. The images in color display the B_1^+ map before and after optimization over the heart. Lower right shows the resulting cardiac image at 7T. TR/TE=45/3.06 ms; 2.0 x 2.0 x 5.5 mm resolution; Matrix size 144 x 192; Breath held and ECG retrogated; Snyder, et. al. MRM 61, 517 (2009); Vaughan, et. al. MRM 61, 244 (2009)

for some time; however, they are typically very long when applied with a single transmit channel and as such not practical in most human applications. The use of pTx capability, however, enables the spatial encoding to be performed in part by the coil transmit sensitivity profiles, leading to a significant shortening of the pulse. This shortening, however, results in substantial increases in peak voltage that must be used, and hence SAR. Strategies to control this SAR amplification are pursued in several laboratories and will be critical in successfully using this approach. The number of channels employed likely plays an important role in SAR deposition with pTx applications. Just as in spatial encoding with multichannel receive to replace k-space encoding [15–17], spatial encoding to shorten the k-space trajectory in spatially targeted RF pulses works much more efficiently as the relative object size gets larger. Thus, the acceleration factors that can be achieved to shorten otherwise extremely long, and, as such, impractical pulses also improve with higher magnetic fields and with a larger object size. Thus, one solution to the ultra-high field transmit RF non-uniformity problem is actually a strategy that works particularly well in ultra-high fields. Provided that SAR limitations can be overcome, spatially targeted pulses applied using pTx introduces the possibility of applications beyond just B_1 flattening, such as restricted FOV

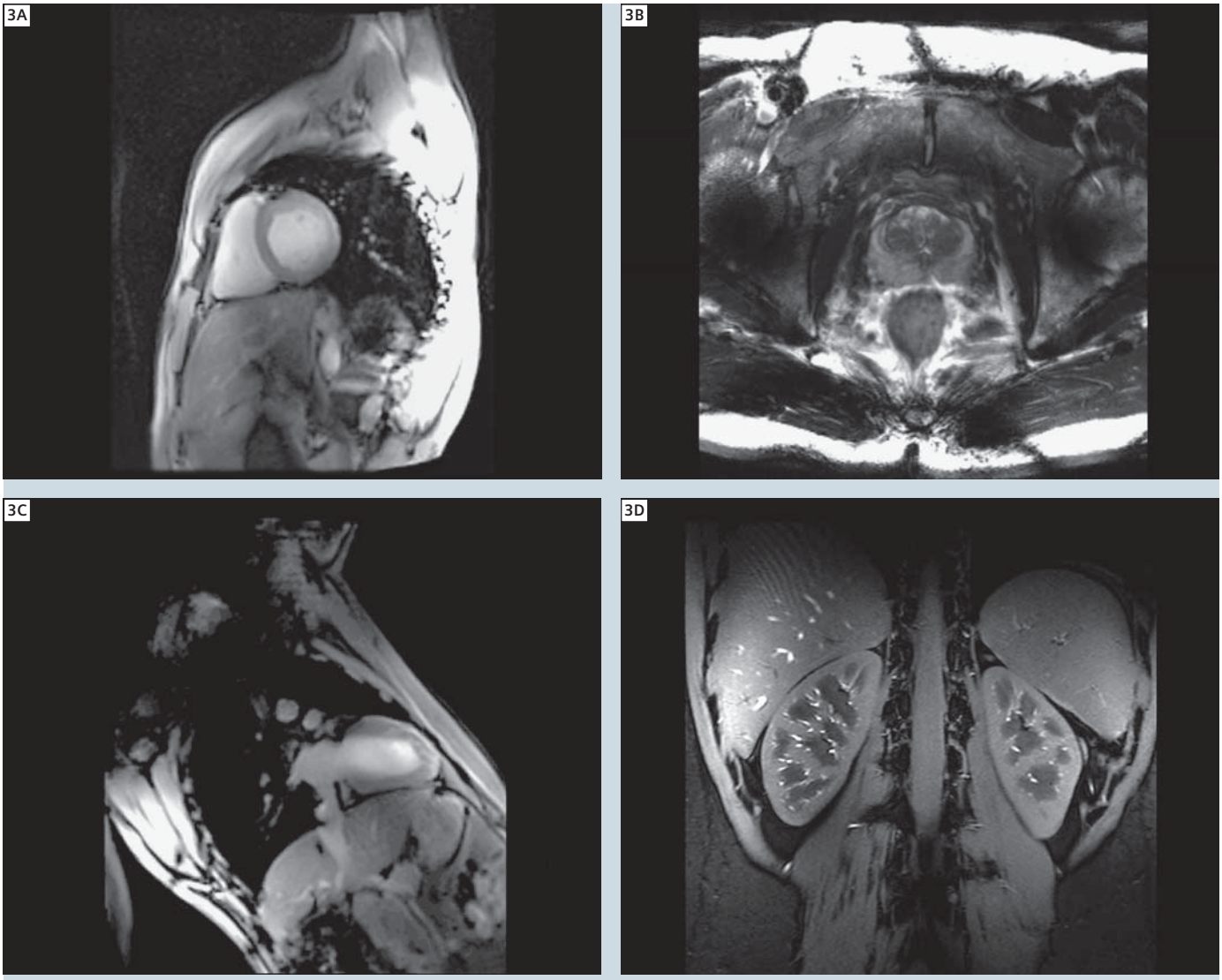

3 7T body images with targeted B_1 shimming using 16-channel pTx capability; cardiac images (on two different planes), a transaxial image through the torso at the level of prostate and a coronal plane through the kidneys obtained using pTx and multichannel receive technology. Note that while there exists strong non-uniformities in the entire image, the image over the targeted organ(s) (heart, prostate and kidneys) is relatively uniform.

"zoomed" imaging, vessel selective angiography etc.
These initial results are a prelude to dramatic improvements that are sure to come in body imaging using pTx methodology and enabling the exploitation of advantages provided by ultrahigh fields, such as improved SNR, improved contrast in many instances, longer T1 times of blood, and improved parallel imaging. In particular, many SNR limited applications in the body, such as angiography and perfusion imaging without using an exogenous contrast agent, vessel wall imaging, high resolution imaging of pathology and of musculoskeletal structures and high resolution spectroscopy, to name a few potential applications, will come to exist and will be further enhanced even at higher magnetic fields. Finally, it is inevitable that these successes will impact, in some fashion, how we do body imaging at the lower magnetic field of 3 or even 1.5T.

Contact
Professor Kamil Ugurbil, Ph.D.
Center for Magnetic Resonance Research
Dept. of Radiology
University of Minnesota
Minneapolis, 55455
USA
kamil@cmrr.umn.edu

References

1 Ugurbil, K., G. Adriany, P. Andersen, W. Chen, M. Garwood, R. Gruetter, P.G. Henry, S.G. Kim, H. Lieu, I. Tkac, T. Vaughan, P.F. Van De Moortele, E. Yacoub, and X.H. Zhu, *Ultrahigh field magnetic resonance imaging and spectroscopy. Magn Reson Imaging,* 2003. 21(10): p. 1263–81.

2 Ugurbil, K., L. Toth, and D.S. Kim, *How accurate is magnetic resonance imaging of brain function?* Trends Neurosci, 2003. 26(2): p. 108–14.

3 Harel, N., K. Ugurbil, K. Uludag, and E. Yacoub, *Frontiers of brain mapping using MRI.* J Magn Reson Imaging, 2006. 23(6): p. 945–57.

4 Ugurbil, K., G. Adriany, C. Akgün, P. Andersen, W. Chen, M. Garwood, R. Gruetter, P.-G. Henry, M. Marjanska, S. Moeller, P.-F. Van de Moortele, K. Prüssmann, I. Tkac, J.T. Vaughan, F. Wiesinger, E. Yacoub, and X.-H. Zhu, *High Magnetic Fields for Imaging Cerebral Morphology, Function and Biochemistry, in Biological Magnetic Resonance: Ultra High Field Magnetic Resonance Imaging*, P.M.L. Robitaille, and Berliner, L.J., Editor. 2006, Springer: New York. p. 285–342.

5 Ugurbil, K., W. Chen, N. Harel, P.-F. Van de Moortele, E. Yacoub, X.H. Zhu, and K. Uludag, *Brain Function, Magnetic Resonance Imaging of, in Wiley Encyclopedia of Biomedical Engineering*, M. Akay, Editor. 2006, John Wiley & Sons, Inc: Hoboken. p. 647–668.

6 Vaughan, J.T., M. Garwood, C.M. Collins, W. Liu, L. DelaBarre, G. Adriany, P. Andersen, H. Merkle, R. Goebel, M.B. Smith, and K. Ugurbil, *7T vs. 4T: RF power, homogeneity, and signal-to-noise comparison in head images.* Magn Reson Med, 2001. 46(1): p. 24–30.

7 Duyn, J.H., P. van Gelderen, T.Q. Li, J.A. de Zwart, A.P. Koretsky, and M. Fukunaga, *High-field MRI of brain cortical substructure based on signal phase.* Proc Natl Acad Sci U S A, 2007. 104(28): p. 11796–801.

8 Rooney, W.D., G. Johnson, X. Li, E.R. Cohen, S.G. Kim, K. Ugurbil, and C.S. Springer, Jr., *Magnetic field and tissue dependencies of human brain longitudinal 1H2O relaxation in vivo.* Magn Reson Med, 2007. 57(2): p. 308–18.

9 Yacoub, E., A. Shmuel, N. Logothetis, and K. Ugurbil, *Robust detection of ocular dominance columns in humans using Hahn Spin Echo BOLD functional MRI at 7 Tesla.* Neuroimage, 2007. 37(4): p. 1161–77.

10 Cho, Z.H., C.K. Kang, J.Y. Han, S.H. Kim, K.N. Kim, S.M. Hong, C.W. Park, and Y.B. Kim, *Observation of the lenticulostriate arteries in the human brain in vivo using 7.0T MR angiography.* Stroke, 2008. 39(5): p. 1604–6.

11 Yacoub, E., N. Harel, and K. Ugurbil, *High-field fMRI unveils orientation columns in humans.* Proc Natl Acad Sci U S A, 2008. 105(30): p. 10607–12.

12 Barfuss, H., H. Fischer, D. Hentschel, R. Ladebeck, A. Oppelt, R. Wittig, W. Duerr, and R. Oppelt, *In vivo magnetic resonance imaging and spectroscopy of humans with a 4 T whole-body magnet.* NMR Biomed, 1990. 3(1): p. 31–45.

13 Yang, Q.X., J. Wang, X. Zhang, C.M. Collins, M.B. Smith, H. Liu, X.H. Zhu, J.T. Vaughan, K. Ugurbil, and W. Chen, *Analysis of wave behavior in lossy dielectric samples at high field.* Magn Reson Med, 2002. 47(5): p. 982–989.

14 Van de Moortele, P.F., C. Akgun, G. Adriany, S. Moeller, J. Ritter, C.M. Collins, M.B. Smith, J.T. Vaughan, and K. *Ugurbil, B(1) destructive interferences and spatial phase patterns at 7 T with a head transceiver array coil.* Magn Reson Med, 2005. 54(6): p. 1503–18.

15 Ohliger, M.A., A.K. Grant, and D.K. Sodickson, *Ultimate intrinsic signal-to-noise ratio for parallel MRI: electromagnetic field considerations.* Magn Reson Med, 2003. 50(5): p. 1018–30.

16 Wiesinger, F., P.F. Van de Moortele, G. Adriany, N. De Zanche, K. Ugurbil, and K.P. Pruessmann, *Parallel imaging performance as a function of field strength--an experimental investigation using electrodynamic scaling.* Magn Reson Med, 2004. 52(5): p. 953–64.

17 Wiesinger, F., P.F. Van de Moortele, G. Adriany, N. De Zanche, K. Ugurbil, and K.P. Pruessmann, *Potential and feasibility of parallel MRI at high field.* NMR Biomed, 2006. 19(3): p. 368–78.

18 Vaughan, J.T., C.J. Snyder, L.J. DelaBarre, P.J. Bolan, J. Tian, L. Bolinger, G. Adriany, P. Andersen, J. Strupp, and K. Ugurbil, *Whole-body imaging at 7T: preliminary results.* Magn Reson Med, 2009. 61(1): p. 244–8.

19 Vaughan, J., RF coil for imaging system. 2003: USA patent 6,633,161.

20 Adriany, G., P.F. Van de Moortele, F. Wiesinger, S. Moeller, J.P. Strupp, P. Andersen, C. Snyder, X. Zhang, W. Chen, K.P. Pruessmann, P. Boesiger, T. Vaughan, and K. Ugurbil, *Transmit and receive transmission line arrays for 7 Tesla parallel imaging.* Magn Reson Med, 2005. 53(2): p. 434–445.

21 Vaughan, J., G. Adriany, K. Ugurbil, J. Strupp, and P. Andersen, *University of Minnesota, assignee. Parallel Transceiver for Nuclear Magnetic Resonance System.* 2005, University of Minnesota: USA 6,969,992.

22 Vaughan, T., L. DelaBarre, C. Snyder, J. Tian, C. Akgun, D. Shrivastava, W. Liu, C. Olson, G. Adriany, J. Strupp, P. Andersen, A. Gopinath, P.F. van de Moortele, M. Garwood, and K. Ugurbil, *9.4T human MRI: preliminary results.* Magn Reson Med, 2006. 56(6): p. 1274–82.

23 Metzger, G.J., C. Snyder, C. Akgun, T. Vaughan, K. Ugurbil, and P.F. Van de Moortele, *Local B_1^+ shimming for prostate imaging with transceiver arrays at 7T based on subject-dependent transmit phase measurements.* Magn Reson Med, 2008. 59(2): p. 396–409.

24 Snyder, C.J., L. DelaBarre, G.J. Metzger, P.F. van de Moortele, C. Akgun, K. Ugurbil, and J.T. Vaughan, *Initial results of cardiac imaging at 7 Tesla.* Magn Reson Med, 2009. 61(3): p. 517–24.

25 Setsompop, K., L.L. Wald, V. Alagappan, B. Gagoski, F. Hebrank, U. Fontius, F. Schmitt, and E. Adalsteinsson, *Parallel RF transmission with eight channels at 3 Tesla.* Magn Reson Med, 2006. 56(5): p. 1163–71.

26 Setsompop, K., V. Alagappan, A.C. Zelinski, A. Potthast, U. Fontius, F. Hebrank, F. Schmitt, L.L. Wald, and E. Adalsteinsson, *High-flip-angle slice-selective parallel RF transmission with 8 channels at 7 T.* J Magn Reson, 2008. 195(1): p. 76–84.

27 Zelinski, A.C., L.L. Wald, K. Setsompop, V. Alagappan, B.A. Gagoski, V.K. Goyal, and E. Adalsteinsson, *Fast slice-selective radio-frequency excitation pulses for mitigating B+1 inhomogeneity in the human brain at 7 Tesla.* Magn Reson Med, 2008. 59(6): p. 1355–64.

28 Wu, X., J.T. Vaughan, K. Ugurbil, and P.F. Van de Moortele, *Parallel excitation in the human brain at 9.4 T counteracting k-space errors with RF pulse design.* Magn Reson Med, 2010. 63(2): p. 524–9.

29 Katscher, U., P. Bornert, C. Leussler, and J.S. van den Brink, *Transmit SENSE.* Magn Reson Med, 2003. 49(1): p. 144–50.

30 Grissom, W.A., C.-Y. Yip, and D.C. Noll, *An image domain approach for the design of RF pulses in transmit SENSE.* Proc. Intl. Soc. Mag. Reson. Med., 2005. 13: p. 19.